



# Novel Polymer Nanocomposites Comprising Triazole Functional Silica for Dental Application

Umar S. Yushau<sup>1</sup> · Lama Almofeez<sup>2</sup> · Ayhan Bozkurt<sup>2</sup>

Received: 31 October 2018 / Accepted: 7 February 2019 / Published online: 22 February 2019  
© Springer Nature B.V. 2019

## Abstract

In the present work, the synthesis of novel nanocomposite polymer resins with silica bearing triazole functional groups was realized. Silica nanoparticles were produced by sol-gel method known as stöber process. Then the surface was modified with 1H-1,2,4-triazole to form functional silica nanoparticles. Dental nanocomposites were produced by insertion of functional nanoparticles into the Bis-GMA/TEGDMA different weight fractions. The initiator system was CQ/EDMAB:0.1:0.4 wt%, and then photopolymerization was carried out by means of LED light having wavelength of 450 nm–500 nm and power density of 1000 mW/cm<sup>2</sup>. FT-IR used to confirm the final structures of the functional nanoparticles as well as nanocomposites. The surface morphology of the materials was analyzed by SEM and thermal properties were studied by TGA. Cytotoxicity test and mechanical test were carried out to evaluate cell viability and mechanical properties of the materials, respectively. Sorption and solubility were conducted on the different formulations to obtain the mean sorption and solubility values of the materials. The test results demonstrated that the composition of the nanocomposite resins significantly changed their properties compared to control samples.

**Keywords** Dental nanocomposites · Nanoparticle · Cytotoxicity · Sorption · Solubility · Mechanical analysis

## 1 Introduction

In dental treatment, polymer composite resins seems to be promising materials have been used for several decades [1, 2]. The interest toward this direction is increasing to solve the drawbacks of long-term performance of this kind of materials in clinical dentistry [3]. The problems related to previous dental resins are poor wear resistance, volumetric shrinkage during polymerization, restoration failure due to inadequate mechanical strength, and stability [4]. The shrinkage leads to marginal leakage, large incidence of secondary dental caries, and high potential for discoloration [5]. These problems greatly affect the longevity of dental composite restoration.

To improve clinical performance of dental composite resins, various attempts have been made since their development on the filler volume and polymer matrix [6]. Determining the filler volume is based on the particle size, silanization, loading [7], and formation of new particles [8, 9]. Particle size and filler volume can greatly influence the physical properties of dental composites [7]. Whereas, examination of the polymer matrix is essentially focused on new monomers formation [10–12]. Polymerization shrinkage decrease as filler volume fraction increase, while hardness, compressive strength, elastic modulus, and flexural strength increase [7].

Filler modifications, which include optimizing filler content [13], packing [14], and hybrid fillers development [15] have been recognized as alternative and effective approaches to increase the performance of polymer based composite resins. Furthermore, growth of nanotechnology applications has shown that incorporating nanomaterials [16–18] in fillers offers advantages such as improving mechanical properties, reducing polymerization shrinkage, and the rate of wear. Presently, the majority of resin-based composites include inorganic nanoparticles to enhance the performance [19]. Nanoparticles have a high specific surface area and rich surface functional groups which are reasons for the improvement

✉ Ayhan Bozkurt  
abozkurt@iau.edu.sa

<sup>1</sup> Department of chemistry, Istanbul University,  
34452 Istanbul, Turkey

<sup>2</sup> Department of Biophysics, IRMC, Imam Abdulrahman bin Faisal  
University, PO Box: 1982, Dammam 31441, Saudi Arabia

**Table 1** Different formulations of resin composites series A

Nanoparticles Type	Series	Wt%
1H-1,2,4-triazole functional silica nanoparticles	A1	10
	A2	20
	A3	30
	A4	40
	A5	50
	A6	60

[20]. Even though nanoparticles have considerable advantages, further progress is needed to achieve long-term satisfactory restorations for clinical therapy [21, 22]. Azole scaffold is still considered as the most viable structure for the production of more effective antimicrobial agents. It has been reported to have remarkable antibacterial activity on methicillin-resistant strains of staphylococcus aureus. However, azoles still have weakness in their spectra, potencies, safety and pharmacokinetic properties. Several attempts have been made to change the structures of the available effective azole drugs to enhance their antimicrobial potency and selectivity [23]. The production of dental composites with multifunctional nanoparticle fillers could be promising for restorative dentistry. It can provide homogeneous distribution in the polymer matrix, compatibility, better percent conversion, improve mechanical properties and increase the lifetime.

In this paper, silica nanoparticles were synthesized via Stöber process and were surface-modified and functionalized with 1H-1,2,4-triazole to form functional silica nanoparticles. Dental nanocomposites were produced by photopolymerization of functional nanoparticle incorporated BisGMA/TEGDMA mixture using an initiator system (CQ/EDMAB). Nanoparticles and nanocomposites were characterized by FT-IR, SEM and TGA. Cytotoxicity test, mechanical analysis, sorption and solubility tests were conducted and interpreted according to control samples.

## 2 Experimental

### 2.1 Materials

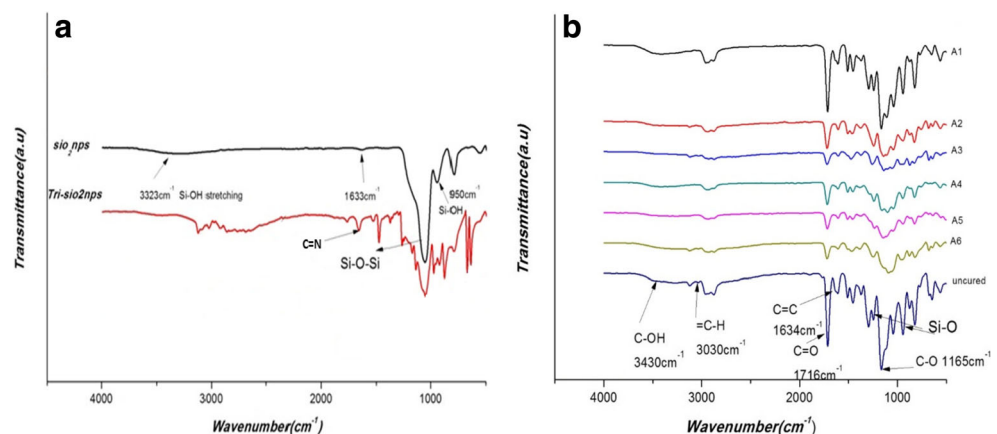
Bis-phenol A glycidyl dimethacrylate, Bis-GMA (>98%), Trimethyleneglycol dimethacrylate, TEGDMA (99%), Camphorquinone (CQ) (Mw = 166.22 g/mol 97%), Dimethylformamide, DMF (99.8% anhydrous), Tetrahydrofuran, THF ( $\geq 99.9\%$ ), Ethanol ( $\geq 99.8\%$  (GC)), Tetraethoxysilane, TEOS (99.999% trace metals basis),  $\text{NH}_4\text{OH}$  (28.0–30.0%  $\text{NH}_3$  basis), Ethyl-4-dimethylamino benzoate, EDMAB ( $\geq 99\%$ ), and 1,2,4-triazole ( $\geq 95\%$  (TLC)), were purchased from Sigma-Aldrich Chemicals. MTT (3-(4,5-dimethylthiazol-2-yl)-2,5-diphenyltetrazolium bromide) and HepG2 cells were obtained from ThermoFisher Scientific.

### 2.2 Sample Preparation

The starting material, silica nanoparticles were produced via typical stöber process from TEOS according to previous work [24–26]. Surface modified silica nanoparticles were synthesized by the reaction of  $\text{nSiO}_2$  with epichlorohydrin with a similar method as mentioned before [27]. The reaction of epichlorohydrin nanosilica occurred in THF. After reaction completion, the modified nanosilica was collected, washed four times with 1:4 ratio of ethanol/ water mixture and kept wet for further reaction.

To synthesize 1H-1,2,4-triazole functional nanosilica, modified epoxy silica nanoparticles were dispersed in 10 ml of dimethylformamide (DMF). Excess amount of the 1H-1,2,4-triazole was included in the reaction system and heated at a temperature of 80 °C [28]. The mixture was stirred under nitrogen environment for 24 h. A solid mixture was formed which was collected and washed four times with 1:4 solution of ethanol and distilled water to remove unreacted remnants. It was then dried in an oven at 80 °C.

**Fig. 1** FT-IR spectra nanosilica and functional silica (a) of composites A series and uncured (b)



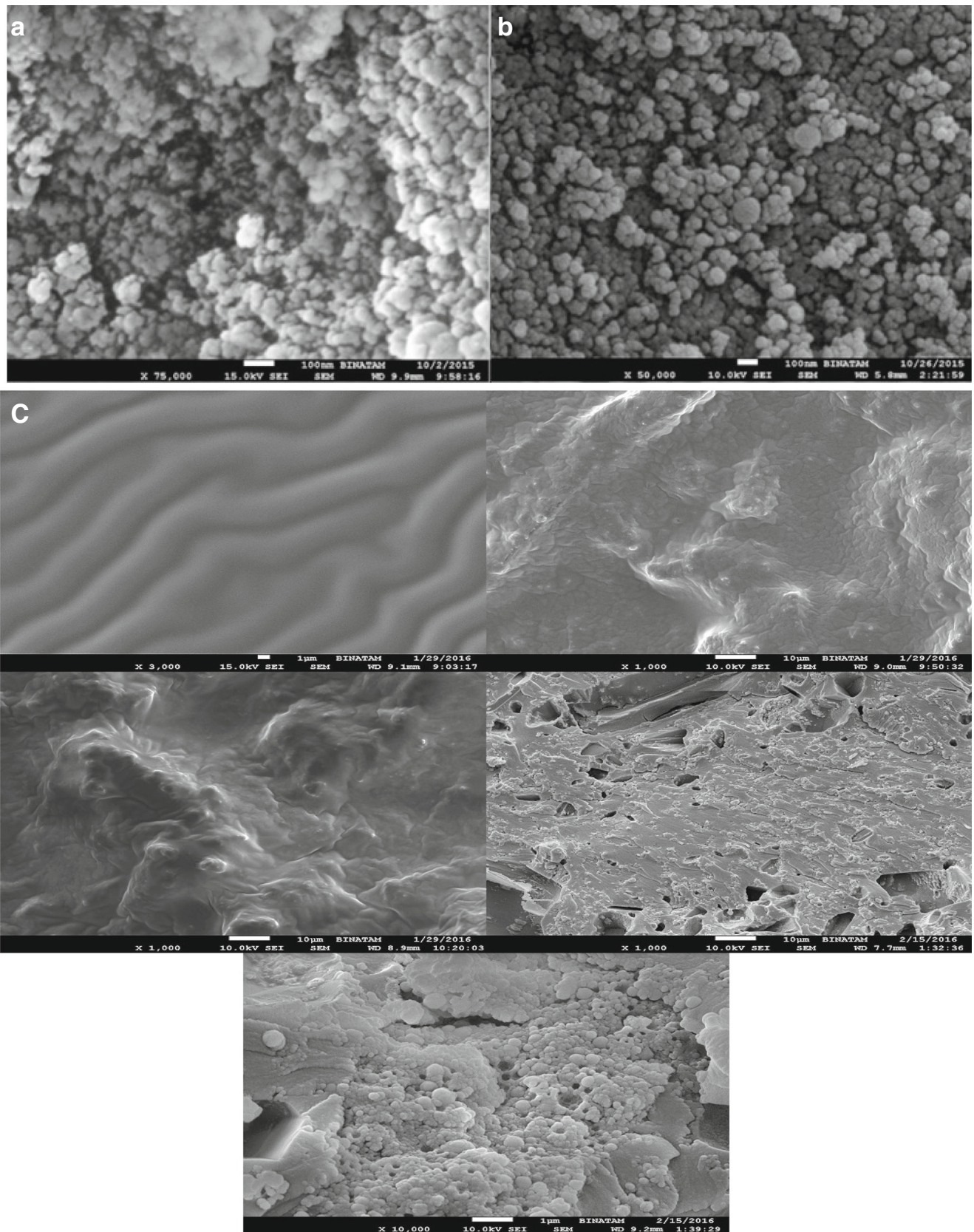
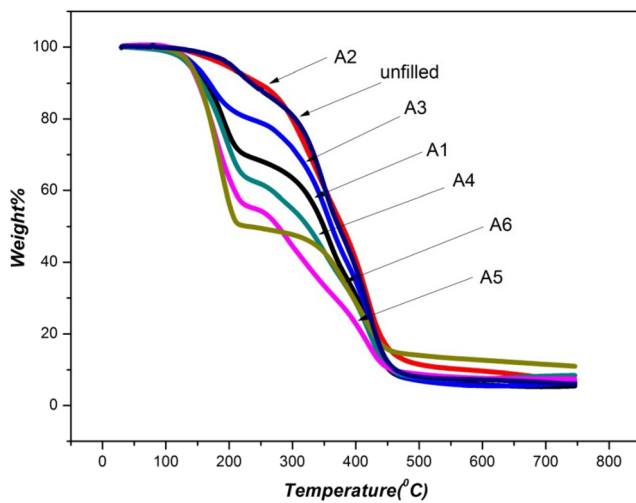


Fig. 2 SEM of nanosilica (a) functional nanosilica (b) the nanocomposite series A20-A60 (c)





**Fig. 3** TGA thermograms of series A and unfilled dental nanocomposites

Nanocomposites were synthesized (series A1–A6) at various weight fractions of the functional nanoparticles. Firstly, the monomers Bis-GMA and TEGDMA (50:50 wt%) were blended by stirring at a temperature of 50 °C. Functional nanosilica was added at different weight percentages ranging from 10% to 60 wt%. The mixing was done by continuous stirring for about 30 min until getting homogenous mixture. This process was followed by insertion of initiator/co-initiator system made up of CQ (0.1 wt%) and EDMAB (0.4 wt%) and then the mixture homogenized by stirring to get transparent mixture. The paste was filled in Teflon mold (5 mm diameter by 3 mm thickness). Photopolymerization was done with a LED light source for 60 s and hard rigid pellets were obtained (Table 1).

### 3 Characterizations

All samples were dried under vacuum and stored in a glove box before FT-IR spectra analysis. The data was recorded in the range 4000–400  $\text{cm}^{-1}$  and a resolution of 4  $\text{cm}^{-1}$  in ATR system with Bruker Alpha-P.

**Table 2** Sorption and solubility values of composite A series

Composite	Sorption value ( $\text{mg}/\text{mm}^3$ )	Solubility value ( $\text{mg}/\text{mm}^3$ )
A1	0.072	0.052
A2	0.088	0.099
A3	0.123	0.068
A4	0.148	0.138
A5	0.138	0.257
A6	0.376	0.570

Thermal stabilities and percentage modification of functionalized fillers and composites were examined by thermogravimetric (TG) analysis with a Perkin Elmer STA 6000. The samples (~5 mg) were heated from room temperature to 700 °C under  $\text{N}_2$  atmosphere at a heating rate of 10°  $\text{C min}^{-1}$ .

Nanoparticle and Nanocomposite surface morphologies were examined by using scanning electron microscope (SEM), *Philips XL30S-FEG*. The samples were gold coated before the SEM analysis. SEM was operated at acceleration voltage of 10 kV.

Mechanical properties of the disc-shaped test specimens with 5 mm diameter and 3 mm thickness were tested in a Universal Testing machine by using a compression fixture. The speed of cross-head was 0.1 mm/min. Stress (MPa)–strain (%) curves were recorded and the mechanical parameters of “Young’s modulus ( $E$ )”, “compression strength or maximum stress”, and “strain at break or failure” were determined.

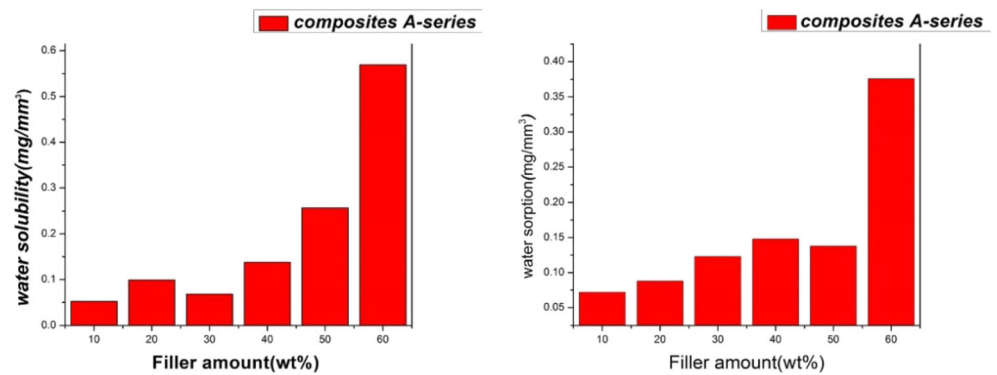
Surface morphologies of the samples were determined using scanning electron microscope with specifications: Philips XL30S-FEG. Also, all samples were gold sputtered before the analysis.

Before solubility and sorption test, cured composite samples were kept to dry in an oven at 37° C for 24 h. These samples were further placed in desiccators to dry for 2 h. For each formulation composition, dried sample were measured severally till a constant mass  $m_0$  was found. The samples were immersed in water in separate sample bottles and kept in an oven at 37° C for 3 weeks. After this period, the samples were taken and rinsed with water. The water from the surface of the specimen was wiped out till there was no visible moisture. These samples were waved in the air for 15 s. Lastly, the samples were weighed. For all the samples the mass ( $m_1$ ) was recorded. The samples were again kept in the desiccators to dry following the same cycle as mention above at the temperature of 58° C. The specimen was weighed again and mass ( $m_2$ ) was obtained. To obtain constant mass for any test sample, the steps was repeated accordingly.

Solubility and sorption tests were carried out to investigate water sorption (A) and water solubility (S) of the dental composites materials in accordance with oysaed & Ruyter 12 formula which is given as  $A = m_1 - m_2/v$  and  $S = m_0 - m_2/v$ , where  $m_1$  is the sample weight before immersion,  $m_1$  is the sample weight after immersion, and  $m_2$  is the sample weight after immersion and desiccation. V is the volume of the specimen in cubic millimeters.

For cytotoxicity studies the dental composites were casted in the form of discs by using Teflon-based mold containing uniformed wells of 3 mm thickness and 5 mm diameter. The control discs of the same measurements were made of Teflon, as well. In the tissue culture hood, the discs were sterilized for 20 min with UV light and transferred into 15 ml conical tube. Sequentially, the specimens were washed with %70 ethanol and deionized water, and left to dry in the hood for 5 min.

**Fig. 4** Water solubility and sorption of composites A series



Each disc was then placed into an individual well of 24-well plate and pre-incubated in 1 ml of DMEM for 15 min.

HepG2 cells (ATCC) were seeded at  $1 \times 10^5$  cells/well in a 24-well plate containing DMEM supplemented with 4.5 g/l glucose, 10% FBS, 2 mM L-glutamine, 100 U/ml penicillin, and 100  $\mu$ g/ml streptomycin. Then, it was pre-incubated

overnight at 37 °C and 5% CO<sub>2</sub>. After that, the cells were added to the discs of various formulations and incubated for 24 h. Following incubation, all wells were washed with 500  $\mu$ L of 1  $\times$  PBS and incubated with 0.3 mg/ml of MTT (3-(4,5-dimethylthiazol-2-yl)-2,5-diphenyltetrazolium bromide) in 1  $\times$  PBS at 37 °C for 3 h. The resulting formazan

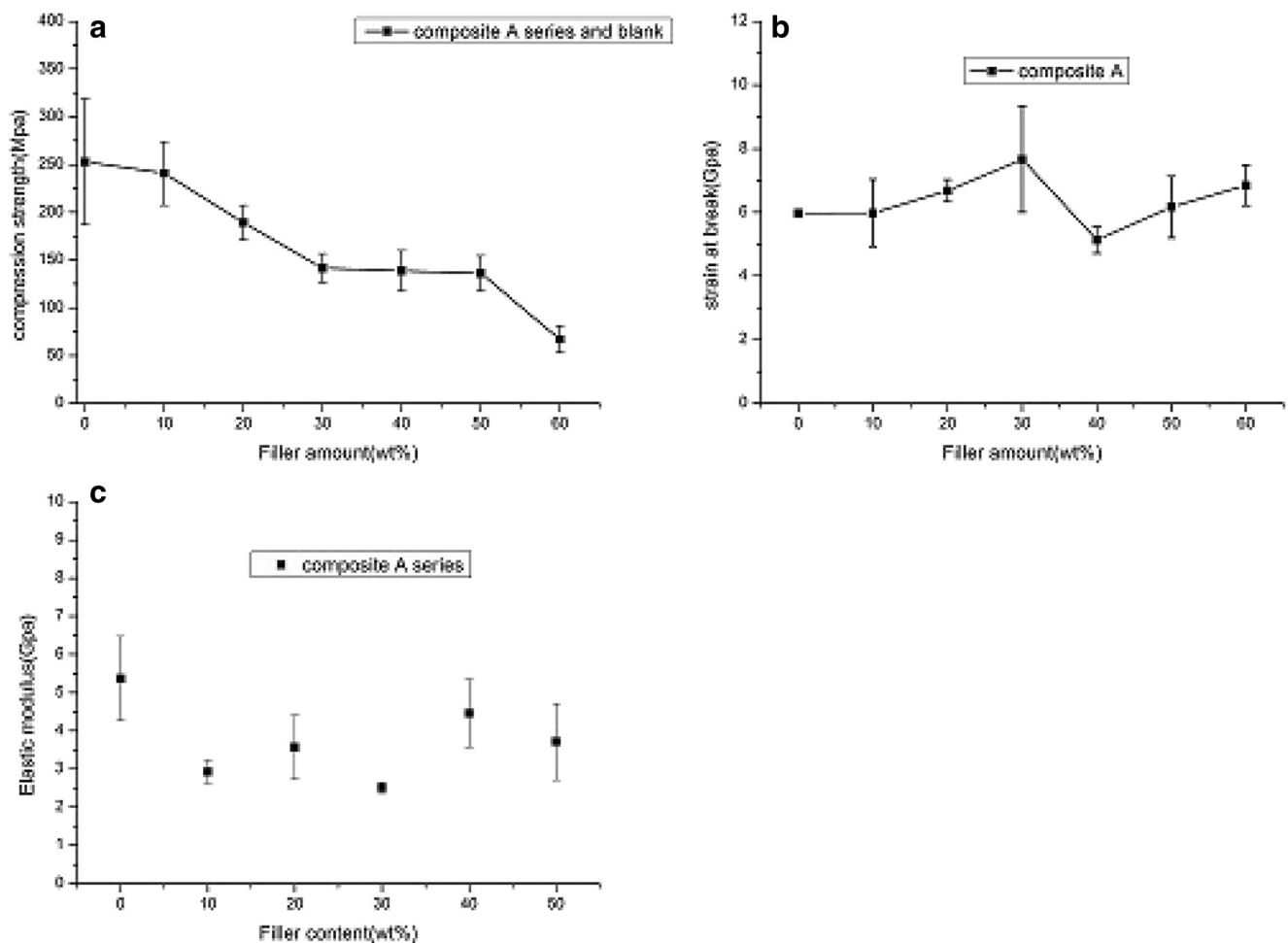


**Fig. 5** Plot of mean & SD values for (a) compression strength, (b) strain at break & (c) elastic modulus for composite A & blank

**Table 3** Mean and standard deviation values of compression strength, strain at break and Elastic Modulus for blank & A composites series

Composites	Filler fraction (wt%)	Compression strength (MPa)	Strain at break (GPa)	Elastic modulus (GPa)
A <sub>0</sub> (blank)	0	253 ± 66	5.975 ± 0.08	5.37 ± 1.1
A1	10	241 ± 33.3	5.98 ± 1.06	2.9 ± 0.30
A2	20	189.33 ± 18.34	6.68 ± 0.35	3.57 ± 0.83
A3	30	141.33 ± 15.31	7.67 ± 1.67	2.5 ± 0.13
A4	40	138.67 ± 21.13	5.13 ± 0.42	4.46 ± 0.89
A5	50	136 ± 18.25	6.17 ± 0.97	3.71 ± 1.01
A6	60	67 ± 14.14	6.85 ± 0.64	4.0 ± 1.36

crystals were solubilized by removing MTT solution and adding 450  $\mu\text{L}$  of DMSO. The absorbance was measured at 570 nm by Thermo Scientific spectrophotometer.

## 4 Results and Discussion

### 4.1 Ft-IR

FT-IR spectra of nano-SiO<sub>2</sub> and functional silica are illustrated Fig. 1a, and dental polymer composite resins are shown in and Fig. 1b. Fig 1a shows absorption peaks appeared at 3332  $\text{cm}^{-1}$  and 1633  $\text{cm}^{-1}$  are assigned to the O-H stretching vibration and O-H distorting vibration, respectively. The broad peak at 1063  $\text{cm}^{-1}$  is attributed to the Si-O-Si formation. The peaks at 1220  $\text{cm}^{-1}$  and 1083 are assigned to the Si-O stretching. After functionalization of nano silica, the absorption peaks at 1420, 1520  $\text{cm}^{-1}$  and 1670  $\text{cm}^{-1}$  belong to azolic ring.

The characteristic groups peaks for dimethacrylate monomers contained in the composite matrix (BisGMA-co-TEGDMA) are found in the FT-IR around 3479  $\text{cm}^{-1}$  (medium, wide) due to C—OH groups of Bis-GMA (vibration due to stretch), while the 3050–3038  $\text{cm}^{-1}$  small peaks are due to the C—H bonds (or the aromatic H). Peaks at 2963–

2850  $\text{cm}^{-1}$  corresponds to —CH<sub>3</sub> and —CH<sub>2</sub> groups (asymmetric and symmetric stretching, strong and sharp) of all monomers. The strong and narrow peak at 1717–1715  $\text{cm}^{-1}$  is due to C=O group of all methacrylates, while the medium, narrow peak at 1637–1635  $\text{cm}^{-1}$  is due to stretch vibration of C=C [29]. An absorbance at 1609–1608  $\text{cm}^{-1}$  is also shown and attributed to the aromatic C=C bonds of Bis-GMA composite matrix. The peaks at 1170–1169  $\text{cm}^{-1}$  is due to C-O bonds in most of the cases. Even lower, the range of 1250–950  $\text{cm}^{-1}$  usually contains the characteristic asymmetric stretching vibrations of the Si-O bonds.

### 4.2 Morphology of Fractured Composites

The SEM images of the nanoparticles and nanocomposite series A20–A60 are illustrated in Fig. 2a–c. Fig. 2a demonstrates silica nanoparticles with size 20–40 nm and Fig. 2b shows triazole functional silica sizes are ranging from 60 to 90 nm. Fig. 2c gives the surface morphology of the composites which are smoother at lower functional nanoparticle contents. Surfaces became rougher as the nanoparticle content increased in the polymer resin. When it reached to 60%, more clear presence of functional nanoparticles was observed. For all the A series nanocomposites, a quite good dispersion and good interfacial adhesion of functional fillers occurred in the crosslinked polymer matrix.

### 4.3 Thermogravimetric Analysis

TGA thermograms of nanocomposite series are illustrated for in Fig. 3. The host matrix and composite materials are stable up to 100 °C. Above this temperature domain, two step decompositions occurred. The first degradation was around 150 °C which can be attributed to degradation of azoles. Percent loss was between 100 and 350 °C and increased with the filler content. The second weight loss above 350 °C that could be attributed to further decomposition of organic matrix and inorganic phase. As investigated previously, the dental resins gave a cross-linked 3-D structure and were highly resistant to thermal decomposition in an inert atmosphere. A great deal of energy is require to break polymer matrix bonds

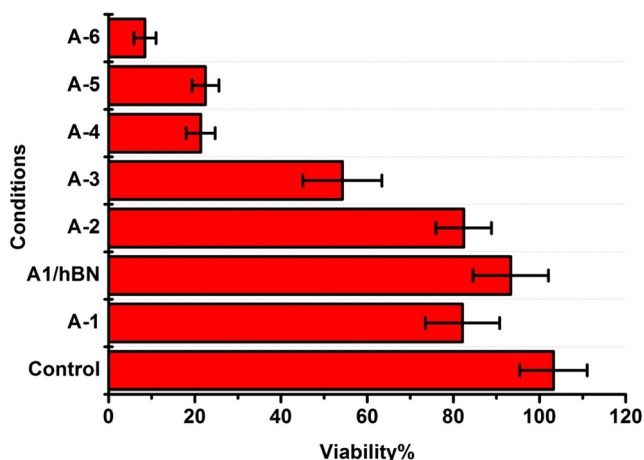


**Fig. 6** Cell viability mean and SD plots of composites A series

[30]. Previously, Vouvoudi et al. reported that decomposition behavior of monomers (Bis-GMA and TEGDMA) are considerably affected by their chemical structure [31].

#### 4.4 Sorption and Solubility of the Composite Electrolytes

The results of sorption and solubility are summarized in Table 2. Analysis of the series of all the composites indicated that an increase in both sorption and solubility properties were detected with an increase in functional nanoparticle content (Fig. 4). As seen, the composite A1 shows the least water sorption of  $72 \mu\text{g}/\text{mm}^3$  which is comparable with the value required for ISO 4049 [32]. Then, sorption values increased slightly with the filler content from A2 to A5. Similarly, solubility values exhibited similar trend at lower contents up to 40% and then increased. These values implied that high solvent sorption resulted in higher solubility after storage in water at  $37^\circ\text{C}$  for 3 weeks.

#### 4.5 Mechanical Analysis

The mean and standard deviation values of compression strength, strain at break and elastic Modulus for blank and composites series A are illustrated in Figs. 5 and also summarized in Table 3. Conventional dental composites which are filled with the hybrid fillers have elastic modulus and the compression strength in the range of 5 to 10 GPa, and 150 to 250 MPa, respectively [33–36]. The mean compression strength values of some of the composites in this work shows a considerable improvement in mechanical properties when compared to dental composites made with hybrid fillers.

Composite A1 has the highest compression strength ( $241 \pm 33.3$  MPa) compared to blank ( $253 \pm 66$  MPa) and it decreased with the additive amount. Whereas, the highest elastic modulus was obtained in composites A4 ( $4.4628 \pm 0.89$  GPa) with respect to Blank ( $5.37 \pm 1.1$  GPa). Moreover, the composites A1, A2 and A3 demonstrated higher strain at break which may be due to denser crosslinking at lower filler content and better interaction between host polymer and functional nano additive.

#### 4.6 Cytotoxicity Test

Cytotoxicity analysis of various formulations reveals potentially toxic and safe candidates. Potent cytotoxicity or its complete absence is equally useful in various applications of dental composites. By increasing the filler amount of different formulations, cellular viability was evaluated using the MTT-based assay by 24 h incubation of cell. To investigate the cytotoxic potential of novel modified silica nanoparticle-based dental composites in vitro, each of the freshly synthesized composites was prepared in the shape of a disc using

mold measuring 5 mm diameter and 3 mm thickness disc and incubated with HepG2 cells. Assessment of viability of cellular was done using assay of MTT followed by 24 h cell incubation for each of the formulations with increasing the concentration. Controls were represented by the same-size discs made of Teflon. As a result, formulations A-1/hBN were non-toxic, whereas, A1- A3, were moderately toxic, and A4, A5, A6, were very toxic compared to the Teflon-made controls, as observed in Fig. 6.

## 5 Conclusions

In the present work, polymer nanocomposite resins comprising various fractions of 1H-1,2,4-triazole modified nanosilica particles were investigated. Functional silica was produced and then homogeneously dispersed in the polymer resin matrix as confirmed by SEM analysis. Thermogravimetric (TGA) results showed an adequate thermal stability of nanocomposite up to at least  $100^\circ\text{C}$ . Water sorption and solubility mean values were increased with the filler amount, i.e., for A1-A6  $0.072\text{--}0.376 \text{ mg}/\text{mm}^3$  and  $0.052\text{--}0.257 \text{ mg}/\text{mm}^3$ , respectively. Cytotoxicity analysis showed that A1, A2, and A3 are moderately toxic, whereas, A4, A5, and A6 are very toxic compared to the Teflon-made controls. The mechanical measurements yielded maximum and minimum values for compression strength ( $241 \pm 33.3$  and  $67 \pm 14.14$  MPa), elastic modulus ( $2.92333 \pm 0.30$  and  $4.00 \pm 1.36$  GPa). The results indicated that there is a decrease in the compression strength and elastic modulus, with increasing the filler content. It was demonstrated that the nanocomposite resins so-called A1-A3 are promising candidates and could be suggested for dental application.

**Publisher's Note** Springer Nature remains neutral with regard to jurisdictional claims in published maps and institutional affiliations.

## References

1. Bowen RL (1963) Properties of a silica-reinforced polymer for dental restorations. *J. Am. Dent. Assoc.* 66:57–64
2. Stein P, Sullivan J, Haubenreich J, Osborne P (2005) Composite resin in medicine and dentistry. *J Long-Term Eff Med Implants* 15(6):641–654
3. T. Aure, P. Anto, M. Se, and A. D. Logue, (2006) A clinical evaluation of posterior composite restorations : 17-year findings, 34: 427
4. Bayne SC, Heymann HO, Swift EJ (1994) Update on dental composite restorations. *J Am Dent Assoc* 125:687–701
5. Rueggeberg FA (2002) From vulcanite to vinyl, a history of resins in restorative dentistry. *J Prosthet Dent* 87:364–379
6. Moszner N, Salz U (2001) New developments of polymeric dental composites. *Prog Polym Sci* 26:535–576

7. Ikejima I, Nomoto R, McCabe JF (2003) Shear punch strength and flexural strength of model composites with varying filler volume fraction, particle size and silanation. *Dent Mater* 19:206–211
8. Ruddell DE, Maloney MM, Thompson JY (2002) Effect of novel filler particles on the mechanical and wear properties of dental composites. *Dent Mater* 18:72–80
9. Xu HHK, Quinn JB, Smith DT, Antonucci JM, Schumacher GE, Eichmiller FC (2002) Dental resin composites containing silica-fused whiskers—effects of whisker-to-silica ratio on fracture toughness and indentation properties. *Biomaterials* 23:735–742
10. Taylor DF, Kalachandra S, Sankarapandian M, McGrath JE (1998) Relationship between filler and matrix resin characteristics and the properties of uncured composite pastes. *Biomaterials* 19:197–204
11. Chung C-M, Kim J-G, Kim M-S, Kim K-M, Kim K-N (2002) Development of a new photocurable composite resin with reduced curing shrinkage. *Dent Mater* 18:174–178
12. Atai M, Nekoomanesh M, Hashemi SA, Amani S (2004) Physical and mechanical properties of an experimental dental composite based on a new monomer. *Dent Mater* 20:663–668
13. Adabo GL, dos Santos Cruz CA, Fonseca RG, Vaz LG (2003) The volumetric fraction of inorganic particles and the flexural strength of composites for posterior teeth. *J Dent* 31:353–359
14. Manhart J, Kunzelmann K-H, Chen HY, Hickel R (2000) Mechanical properties and wear behavior of light-cured packable composite resins. *Dent Mater* 16:33–40
15. Wei Y, Jin D, Wei G, Yang D, Xu J (1998) Novel organic–inorganic chemical hybrid fillers for dental composite materials. *J Appl Polym Sci* 70:1689–1699
16. Xia Y, Zhang F, Xie H, Gu N (2008) Nanoparticle-reinforced resin-based dental composites. *J Dent* 36:450–455
17. Xu HHK, Quinn JB, Smith DT, Giuseppetti AA, Eichmiller FC (2003) Effects of different whiskers on the reinforcement of dental resin composites. *Dent Mater* 19(5):367
18. Fong H (2004) Electrospun nylon 6 nanofiber reinforced BIS-GMA/TEGDMA dental restorative composite resins. *Polymer* 45:2427–2432
19. Wang X, Cai Q, Zhang X, Wei Y, Xu M, Yang X, Ma Q, Cheng Y, Deng X (2016) Improved performance of Bis-GMA/TEGDMA dental composites by net-like structures formed from SiO<sub>2</sub> nanofiber fillers. *Mater. Sci. Eng. C* 59:464–470
20. Mofarreh MR, Shojaosadati SA (2012) Antibacterial properties of pure titanium coated with silver nanoparticles. *Int J Nano Biomater* 4:281
21. Collins CJ, Bryant RW, Hodge K-LV (1998) A clinical evaluation of posterior composite resin restorations: 8-year findings. *J Dent* 26:311–317
22. Ferracane JL (2006) Is the wear of dental composites still a clinical concern?: is there still a need for in vitro wear simulating devices? *Dent Mater* 22:689–692
23. H. Sadeghpour, Y. Ghasemi, Z. Rezaie, and S. Khabnadideh, (2012) Antibacterial Activity of Some New Azole Compounds 8: 267
24. I. A. Rahman et al., (2007) An optimized sol – gel synthesis of stable primary equivalent silica particles 294:102
25. W. Stober and A. Fink, (1968) Controlled Growth of Monodisperse Silica Spheres in the Micron Size Range 1:69:62
26. K. Sreenivasa, K. El-hami, T. Kodaki, and K. Matsushige, (2005) A novel method for synthesis of silica nanoparticles, 289:125
27. C. Alzina, N. Sbirrazzuoli, and A. Mija, (2011) Epoxy-Amine Based Nanocomposites Reinforced by Silica Nanoparticles. Relationships between Morphologic Aspects , Cure Kinetics, and Thermal Properties, 22789
28. U. S. YUSHA'U, (2017) Synthesis and characterization of multifunctional azole silica based nanocomposites for dental application. İstanbul University
29. D. S. Achilias, M. M. Karabela, and I. D. Sideridou, (2008) Thermal degradation of light-cured dimethacrylate resins Part I. Isoconversional kinetic analysis 472:74
30. Vouvoudi EC, Achilias DS, Sideridou ID (2015) Dental light-cured nanocomposites based on a dimethacrylate matrix : thermal degradation and isoconversional kinetic analysis in N<sub>2</sub> atmosphere. *Thermochim Acta* 599:63–72
31. Standard I (2000) ISO 4049 polymer based filling, restorative and luting materials. *Int Organ Stand* 1
32. Samuel SP, Li S, Mukherjee I, Guo Y, Patel AC, Baran G, Wei Y (2009) Mechanical properties of experimental dental composites containing a combination of mesoporous and nonporous spherical silica as fillers. *Dent Mater* 25:296–301
33. Leprince J, Palin W, Mullier T, Devaux J, Vreven J, Leloup G (2010) Investigating filler morphology and mechanical properties of new low-shrinkage resin composite types. *J Oral Rehabil* 37:364–376
34. A. Roman, M. Moldovan, and P. Iuliu, (2012) Study Regarding some Physico-chemical Properties of Composite Resins for Direct Restoration vol. 31, no. 3 pp. 1–8
35. Wang H, Zhu M, Li Y, Zhang Q, Wang H (2011) Mechanical properties of dental resin composites by co- filling diatomite and nanosized silica particles. *Mater Sci Eng C* 31:600–605
36. Cramer NB, Couch CL, Schreck KM, Carioscia JA, Boulden JE, Stansbury JW, Bowman CN (2010) Investigation of thiol-ene and thiol-ene-methacrylate based resins as dental restorative materials. *Dent Mater* 26:21–28